Cold Regions Science and Technology 106–107 (2014) 1–10

Contents lists available at ScienceDirect

Cold Regions Science and Technology

journal homepage: www.elsevier.com/locate/coldregions

A road surface freezing model using heat, water and salt balance and its validation by field experiments

A. Fujimoto [a,*], R.A. Tokunaga [a,1], M. Kiriishi [a,1], Y. Kawabata [a,1], N. Takahashi [a,1], T. Ishida [a,1], T. Fukuhara [b,2]

[a] Traffic Eng. Res. Team, Civil Eng. Res. Inst. for Cold Region, Public Works Rese. Inst., Hiragishi 1-3-1-34, Toyohira-ku, Sapporo 062-8602, Japan
[b] Graduate School of Engineering, University of Fukui, Bunkyo 3-9-1, Fukui 910–8507, Japan

ARTICLE INFO

Article history:
Received 2 October 2013
Accepted 2 June 2014
Available online 9 June 2014

Keywords:
Deicing agents
Road surface freeze prediction model
Heat balance
Water balance
Vehicular liquid dispersion

ABSTRACT

This study aims at helping optimize the application of deicing agents on the winter road surface. In this regard, field tests were conducted for observing how water and deicing agents (= salt) disperse due to passing vehicles as well as for calculating the dissolution rates of salt on the road surface. Additionally, we developed a one-dimensional time-dependent model for the prediction of freezing on a road surface. It takes into account the effects of salting and passing vehicles and is called the RSF-SV model. Its validity was examined by using field test results.

Based on the test results, the relationship between the amount of water dispersed due to passing vehicles and the thickness of the water film on the surface was formulated, and the dissolution rate of salt on the icy road surface was identified. The RSF-SV model used these results for successfully reproducing the time-series changes in the surface temperature, the ice film thickness, the water film thickness, the salt concentration, and the amount of residual salt on the ice-covered road surface after the application of deicing agents.

1. Introduction

In snowy cold regions, application of deicing agents (hereinafter collectively called "salt") is widely implemented as an effective measure against snow damage to road. Salt sprinkled on the road surface helps delay ice formation or melt snow and ice by lowering the freezing point of water on the surface. As the freezing point curve shows, the extent to which ice formation is delayed or snow and ice are melt depends on the concentration and the temperature of the salt solution applied. However, the state of the snow-and-ice covered road surface changes with time in various ways at different places. Even very experienced operators sometimes find it difficult to conduct proper salt application under certain weather conditions. Moreover, many cold regions are now facing some potential factors that may adversely affect proper application of salt on winter roads, including the aging and a decrease in the number of operators and cuts in the budget for road maintenance.

In order to maintain the current winter road safety level, development of technologies for supporting optimal salt application will become increasingly important.

Road surface freeze prediction models have been used for supporting salt application operation. The techniques used in these models depend on either statistical methods or physical methods (i.e. heat balance methods). This study focuses on the latter methods.

Road surface freeze prediction models using a heat balance model were actively developed from 1980 through the 1990s (Rayer, 1987; Sass, 1992; Shao, 1990; Thornes, 1984). Many of these models calculate the heat and water balance on the road surface for determining whether the surface is dry, wet or covered with ice film. The heat and water balance is calculated on the basis of melt, freeze, evaporation, sublimation, rainfall, snowfall and water discharge. In the 2000s, research on these models was conducted at many places in the world and various new models were developed (Bouilloud, 2006; Chapman and Thornes, 2005; Chapman et al., 2001; Crevier and Delage, 2001; Knollhoff et al., 2003; Fujimoto et al., 2008; Greenfield and Takle, 2006; Jansson et al., 2006; Takahashi et al., 2006). It is worthy of mention that road surface freeze prediction models were combined with thermal mapping to make prediction of surface conditions possible along a road or in an area instead of at a fixed-point (Chapman et al., 2001). Some road surface freeze prediction models took into account freezing due to frost that often affects bridges and elevated bridges (Greenfield and Takle, 2006; Knollhoff et al., 2003).

* Corresponding author. Tel.: +81 11 841 1738; fax: +81 11 841 9747.
E-mail addresses: afujimot@ceri.go.jp (A. Fujimoto), roberto-1097ga@ceri.go.jp (R.A. Tokunaga), kiriishi-m22aa@ceri.go.jp (M. Kiriishi), kawabata-y22aa@ceri.go.jp (Y. Kawabata), takahashi-n24k@ceri.go.jp (N. Takahashi), t-ishida@ceri.go.jp (T. Ishida), fukuhara@u-fukui.ac.jp (T. Fukuhara).
[1] Tel.: +81 11 841 1738; fax: +81 11 841 9747.
[2] Tel.: +81 776 27 8595; fax: +81 776 27 8746.

http://dx.doi.org/10.1016/j.coldregions.2014.06.001

One of the remaining challenges for these kinds of models has been the modeling of anthropogenic factors such as the effects of passing vehicles and sprinkled salt. Recently, thermal effects of passing vehicles on the road surface temperature were incorporated in some models (Chapman and Thornes, 2005; Fujimoto et al., 2008; Takahashi et al., 2006). More recently, the researchers of this study proposed a model that takes into account the effects of the stopping and starting of vehicles at signalized intersections (Fujimoto et al., 2012a).

On the other hand, development of models has not been advanced for simulating the effect of salt on the road surface, and very few road surface freeze prediction models take into account the thermal, physical effects of salt on the road surface conditions. If a road surface freeze prediction model that gives consideration to the effects of salt is available, the model will be useful for predicting the surface conditions after salt application as well as for evaluating the effects of salt application, and thus will be able to help optimize salt application operation. The researchers in this study proposed a road surface freeze prediction model that factored in freezing point depression due to salt. The model was validated in laboratory experiments with regard to the prediction of the freezing process of salt solution under limited weather conditions without traffic (Fujimoto et al., 2012b). In order to apply this model to actual roads, it is necessary to develop a model of simultaneous phase transition of water, ice and salt, a process that involves salt dissolution, and also to quantify the movement of salt on the road surface.

To address these issues, this study aims at:

(i) Evaluating the water and salt transfer on the road surface due to passing vehicles;
(ii) Identifying the effects of the dissolution rate of salt on snow and ice on the surface;
(iii) Developing a Road Surface Freeze prediction model that takes into account the effects of Salting and passing Vehicles (RSF-SV model) that utilizes heat, water and salt balance for analysis and is available for analyzing time-series changes in the thickness of the water/ice film, the salt concentration and the amount of residual salt after spraying solid-phase salt on the road surface; and
(iv) Evaluating the validity of the RSF-SV model in the light of the results of field tests that are conducted for examining the effects of sprinkled salt and passing vehicles.

2. RSF-SV model

2.1. Outline of the RSF-SV model

The RSF-SV model can calculate the time change of the temperature, of the mass of water, ice and salt, and of the thickness and salt concentration of the ice layer on the road surface after salt application in one dimension. This model is innovative in that it combines the effects of salt application (i.e. latent heat and freezing point depression) with conventional road surface freeze prediction models that depend on the heat and water balance on the road surface. This model takes into account the thermal effects given by passing vehicles (i.e. frictional heat flux of tires, radiant heat flux of vehicles, sensible heat flux induced by vehicles, and radiant heat shield by vehicles) and physical effects (i.e. dispersion of salt and water).

Modeling of the simultaneous phase transition of water, ice and salt that takes place after salt application to the ice-covered road surface is shown in Fig. 1. Input factors required for analysis are weather conditions (air temperature, relative humidity, wind velocity, insolation flux, sky radiation flux), traffic condition (hourly traffic volume, vehicle speed), road condition (configuration, thermophysical properties, gradient) and the pavement or ground temperature as the bottom boundary condition. When salt is sprinkled over the ice-covered surface, the simultaneous phase transition as shown in Steps 1–4 in Fig. 1 occurs.

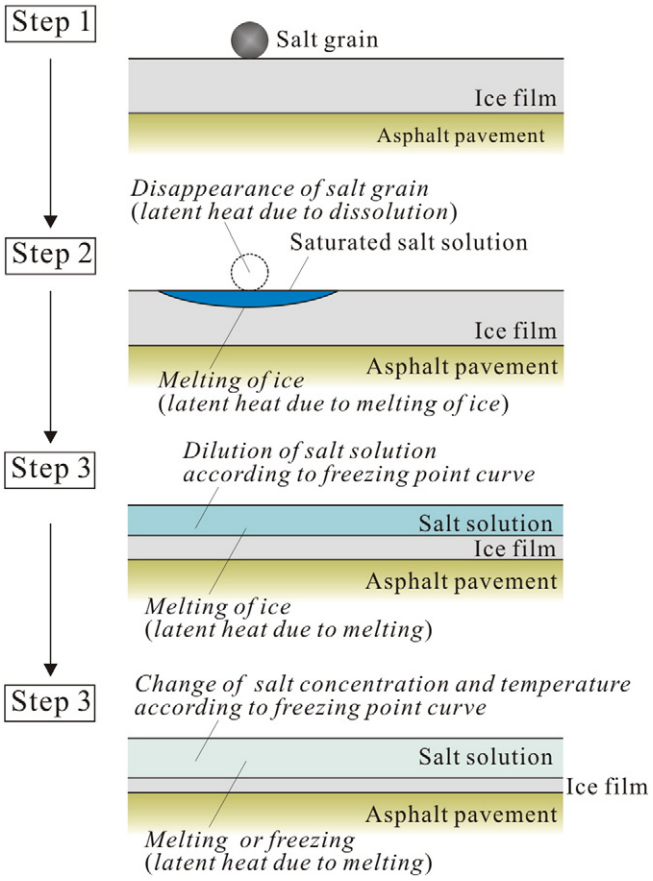

Fig. 1. Phase transition due to salt application to the ice-covered road surface.

Step 1: Salt grains come in contact with the ice film.
Step 2: Saturated salt solution generates around salt grains. During the phase transition, the heat of salt dissolution (i.e. heat absorption by sodium chloride and heat generation by calcium chloride) and heat of ice melting are generated.
Step 3: Ice is melted until the salt solution reaches the concentration level at the freezing temperature, and the salt solution is diluted.
Step 4: When the temperature of the salt solution changes due to the heat balance, the concentration of the salt solution changes according to the freezing point curve, and consequently the ice on the surface is melted or water is frozen.

The RSF-SV model predicts the changes in the temperature and the concentration of the salt solution in the process from Step 1 to Step 4 above by analyzing the heat, water, ice and salt balance on the road surface. With this model, it is possible to obtain data on the thickness of the ice/water film, the concentration of salt, and the amount of residual salt on the road surface. The heat, water, ice and salt balance will be explained in Section 3 below.

2.2. Assumptions

The RSF-SV model is based on the following assumptions:

(I) The dissolution flux of salt is constant in time. Technically speaking, the value of the dissolution flux on the ice surface depends on the area of contact between solid salt grains and salt solution as well as on the surrounding salt solution concentration.

Because the size and shape of salt grains change randomly in a complex way, it is difficult to accurately calculate the area of contact between solid salt grains and salt solution. In this paper, the value of the dissolution flux is determined such that calculation results are consistent with the measurement results. The relationships between values of dissolution flux and the calculation results are examined in 5.4 below;

(ii) Under the conditions of the tests and analyses in this study, heat transfer in longitudinal and traverse directions is not taken into account because vertical heat transfer excels horizontal heat transfer;

(iii) Time intervals at which a vehicle passes by are determined by assuming that the hourly traffic volume is uniformly distributed;

(iv) All vehicles travel along the same track on the road; and,

(v) Wear of the ice film and dispersion of solid salt due to passing vehicles are not taken into account.

3. Theoretical considerations

3.1. Components of an ice layer on the road surface

Fig. 2 is a conceptual diagram showing heat, water, ice and salt transfer on the ice-covered road surface after salt application. The ice layer on the road surface consists of water, ice and salt although some impurities are actually contained. This ice layer is called a WIS layer. The mass per unit area of the WIS layer M_{wis} (kg m^{-2}) is the sum of the mass of water M_w (kg m^{-2}), the mass of ice M_i (kg m^{-2}) and the mass of salt M_s (kg m^{-2}) as expressed by the formula below:

$$M_{wis} = M_w + M_i + M_s. \tag{1}$$

M_s consists of the mass of solid-phase salt M_{ss} (kg m^{-2}) and the mass of liquid-phase salt M_{sl} (kg m^{-2}) dissolved in solvents.

3.2. Material balance

3.2.1. Ice balance

As shown in Fig. 2, the ice balance of the WIS layer is defined by the snowfall flux m_{if} (kg m^{-2} s^{-1}), the sublimation flux m_{il} (kg m^{-2} s^{-1}), the melting and freezing flux m_{wi} (kg m^{-2} s^{-1}) and the flux of ice loss (i.e. dispersion and wear of ice) due to passing vehicles m_{iv} (kg m^{-2} s^{-1}). Thus, the time rate of change in M_i is expressed by the following formula:

$$\frac{\partial M_i}{\partial t} = f(t)m_{if} + m_{il} - m_{wi} + g(t)m_{iv}. \tag{2}$$

In the formula above, t is time (s), and $f(t)$ and $g(t)$ are discriminant variables of the flux that is generated and lost due to passing vehicles. When the road surface is covered by a moving vehicle, then $f(t) = 0$ and $g(t) = 1$, and when the road surface is not covered by a moving vehicle, then $f(t) = 1$ and $g(t) = 0$.

The value of m_{if} is the product of snowfall intensity v_{fi} (m s^{-1}) and snow density ρ_{snow} (kg m^{-3}) as shown in the following formula:

$$m_{if} = v_{fi}\rho_{snow}. \tag{3}$$

The value of m_{il} is given by the following bulk formula:

$$m_{il} = \alpha_{il}(\rho_{va} - \rho_{vs})\theta_i. \tag{4}$$

In the formula above, α_{il} is the bulk sublimation coefficient (m s^{-1}), ρ_{va} and ρ_{vs} are the atmospheric water vapor concentration and the road surface water vapor concentration (kg m^{-3}) respectively, and θ_i (−) is the ice content by mass ($= M_i / (M_w + M_i)$). Regarding this formula, α_{il} is given by the following empirical formula as a function of horizontal wind velocity v_{ws} (m s^{-1}) (Fujimoto et al., 2006):

$$\alpha_{il} = 5.6v_{ws}^{0.7} + 2.2. \tag{5}$$

The value of m_{wi} is positive and snow/ice melts when $T_{wis} \geq$ freezing point T_f (°C) and $M_i > 0$. The value of m_{wi} is negative and snow/ice freezes when $T_{wis} < T_f$ and $M_w > 0$. The value of m_{wi} is defined by the net heat balance of the WIS layer q_{net} (W m^{-2}: formula (18)), and is given by the following formula:

$$m_{wi} = \frac{1}{1000}\frac{q_{net}}{L_{wi}}. \tag{6}$$

In the formula above, L_{wi} is the latent heat of melting and freezing (kJ kg^{-1}).

As stated in 2.2(v) above, m_{iv} is assumed to be zero.

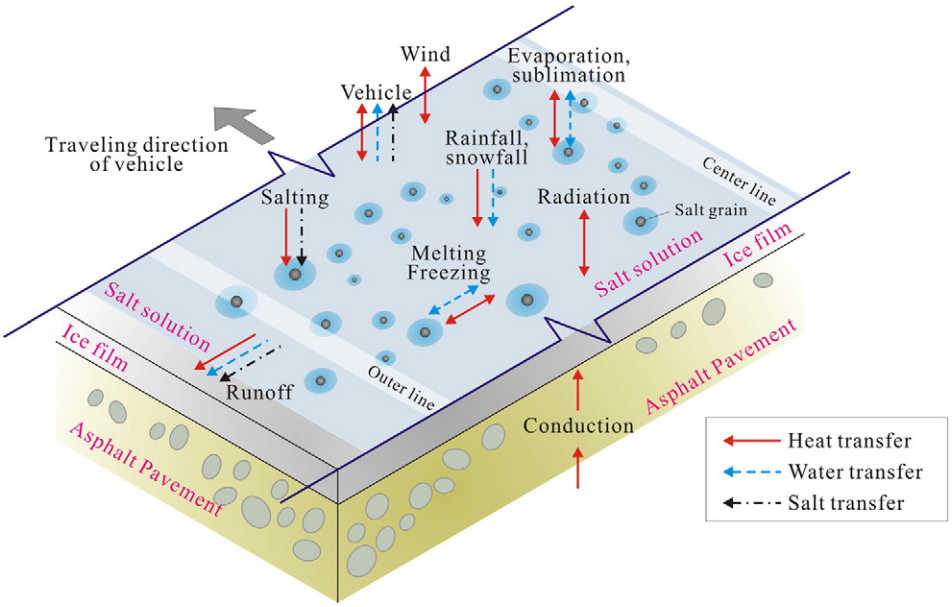

Fig. 2. Heat, water, ice and salt transfer on the ice-covered road surface after salt application.

3.2.2. Water balance

The water balance of the WIS layer is defined by the rainfall flux m_{wf} (kg m^{-2} s^{-1}), the flux of evaporation and condensation m_{wl} (kg m^{-2} s^{-1}), m_{wi}, the flux of road drainage m_{wr} (kg m^{-2} s^{-1}), and the flux of water dispersion due to passing vehicles m_{wv} (kg m^{-2} s^{-1}). Accordingly, the time rate of change in M_w is given by the following formula:

$$\frac{\partial M_w}{\partial t} = f(t)m_{wf} + m_{wl} + m_{wi} + m_{wr} + g(t)m_{wv}. \tag{7}$$

The value of m_{wf} is the product of the rainfall intensity v_{fw} (m s^{-1}) and the water density ρ_w (kg m^{-3}).

$$m_{wf} = v_{fw}\rho_w \tag{8}$$

The value of m_{wl} is given by the following bulk formula:

$$m_{wl} = \alpha_{wl}\{\rho_{va} - \rho_{vs}(1-\phi)\}(1-\theta_i). \tag{9}$$

In the formula above, α_{wl} is the bulk coefficient of evaporation and condensation (m s^{-1}) and ϕ is the ratio of the saturation vapor density over a solution to the saturation vapor density over pure water (−). The value of α_{wl} is given by formula (10) (Fujimoto et al., 2006).

$$\alpha_{wl} = 7.4 \times 10^{-3} V_{ws}^{0.7} + 0.4 \times 10^{-2} \tag{10}$$

ϕ increases in proportion to the salt concentration, being expressed as a linear function of the salt concentration C (−) (He et al., 2003) in the following formula:

$$\phi = 5.1 \times 10^{-4} C. \tag{11}$$

The value of m_{wr} is given in the following formula using the coefficient of runoff velocity k (s^{-1}) and the critical water film thickness on the surface V_{wc} (m^3 m^{-2}) (Sass, 1992):

$$m_{wr} = k(V_{wc} - V_w)\rho_w. \tag{12}$$

The following values were used in this study: $k = 0.003$ s^{-1}, and $V_{wc} = 0.0005$ m^3 m^{-2} = 0.5 mm (Sass, 1992). When $V_{wc} > V_w$ applies, $m_{wr} = 0$.

Regarding m_{wv}, water dispersion due to a passing vehicle m_{wv}' (kg m^{-2} passing vehicle^{-1}) was obtained on the basis of field test results, and m_{wv} is given in the following formula on the assumption that m_{wv}' takes place in a short time Δt_v (s passing vehicle^{-1}):

$$m_{wv} = -\frac{m_{wv}'}{\Delta t_v}. \tag{13}$$

m_{wv}' will be explained in detail in 4.2.2 below.

3.2.3. Solid-phase salt balance

The solid-phase salt balance in the WIS layer is defined by the salt spreading flux m_{sf} (kg m^{-2} s^{-1}), the dissolving flux m_{sl} (kg m^{-2} s^{-1}) and the flux of solid-phase salt dispersion due to passing vehicles m_{ssv} (kg m^{-2} s^{-1}). The time rate of change in the M_{ss} is given by the following formula:

$$\frac{\partial M_{ss}}{\partial t} = m_{sf} - m_{sl} + g(t)m_{ssv}. \tag{14}$$

The values of m_{sl} are quantified in 5.4 below. As assumed in 2.2 (v), the value of m_{ssv} is fixed at zero.

3.2.4. Liquid-phase salt balance

The liquid-phase salt balance in the WIS layer is defined by m_{sl}, the flux of salt discharged from the road surface m_{sr} (kg m^{-2} s^{-1}), and the flux of salt loss due to passing vehicles (i.e. dispersion into the atmosphere and adherence to vehicle bodies) m_{sv} (kg m^{-2} s^{-1}). The time rate of change in M_{sl} is given by formula (15) below:

$$\frac{\partial M_{sl}}{\partial t} = m_{sl} + m_{sr} + g(t)m_{sv}. \tag{15}$$

Because m_{sr} and m_{sv} are associated with water transfer, they are given by the following formulae using m_{wr} and m_{wv} respectively:

$$m_{sr} = \frac{C}{1-C}m_{wr} \tag{16}$$

$$m_{sv} = \frac{C}{1-C}m_{wv}. \tag{17}$$

3.3. Heat balance

3.3.1. WIS layer on the road surface

The heat balance of the WIS layer as illustrated in Fig. 2 is calculated by formula (18) below:

$$\frac{\partial}{\partial t}\{(\rho c)_{wis}V_{wis}T_{wis}\} = q_{csp} + q_{rn} + q_{sn} + q_{ln} + q_{vn} = q_{net}. \tag{18}$$

In this formula, $(\rho c)_{wis}$ is the volumetric heat capacity of the WIS layer (J m^{-3} K^{-1}), V_{wis} is the volume of the WIS layer (m^3 m^{-2}), T_{wis} is the temperature of the WIS layer (°C), q_{csp} is the flux of pavement heat (i.e. the heat conducted between the WIS layer on the road surface and the pavement) (W m^{-2}), q_{rn} is the flux of net radiant heat (W m^{-2}), q_{sn} is the flux of net sensible heat (W m^{-2}), q_{ln} is the flux of net latent heat (W m^{-2}), and q_{vn} is the flux of net vehicle heat (W m^{-2}). The value of $(\rho c)_{wis}$ is a harmonic mean of the volumetric heat capacity of water, ice and salt in the snow-and-ice layer on the road surface.

The value of q_{csp} is calculated by formula (19) using the thermal contact resistance r_c (m^2 K W^{-1}) generated in the interface between the pavement surface and the WIS layer:

$$q_{csp} = \frac{1}{\frac{V_{wis}/2}{\lambda_{wis}} + \frac{V_{ps}/2}{\lambda_p} + r_c}\left(T_{ps} - T_{wis}\right). \tag{19}$$

In this formula, λ_{wis} is the thermal conductivity of the WIS layer (W m^{-1} K^{-1}), λ_p is the thermal conductivity of pavement (W m^{-1} K^{-1}), V_{ps} is the thickness of the pavement surface elemental layer (m^3 m^{-2}), and T_{ps} is the representative temperature of the pavement layer (°C) which means the temperature of pavement $V_{ps}/2$ below the interface between the WIS layer and the pavement layer. The value of r_c is given by the following formula according to Fujimoto et al. (2007):

$$r_c = 0.6 \times 10^{-3} \exp(5.3\theta_a). \tag{20}$$

In this formula, θ_a is the air content by volume in the WIS layer (−). Under the test conditions in this study, $\theta_a = 0$ and thus $r_c = 0.6 \times 10^{-3}$ m^2 K W^{-1}. The value of λ_{wis} is a harmonic mean of the thermal conductivity of water, ice and salt in the WIS layer.

The value of q_{rn} is the sum of the flux of long-wave radiation on the road surface q_{rlu} (W m^{-2}), the flux of long-wave sky radiation q_{rld} (W m^{-2}), the flux of short-wave radiation q_{rsd} (W m^{-2}) and the

reflection component q_{rsu} (W m^{-2}) of q_{rsd} as shown in the following formula:

$$q_{rn} = f(t)q_{rld} - q_{rlu} + f(t)q_{rsd} - q_{rsu}. \quad (21)$$

Following *Stefan–Boltzmann* law, the value of q_{rlu} is given by the following formula:

$$q_{rlu} = \varepsilon_{wis}\sigma(T_{wis} + 273.15)^4. \quad (22)$$

In this formula, σ is the *Stefan–Boltzmann* constant (W m^{-2} K^{-4}) and ε_{wis} is the emissivity of the WIS layer surface (−). The value of ε_{wis} is a harmonic mean of the emissivity of water and ice (=0.96 and 0.98) (Cengel, 1998) in the WIS layer. Measured values are given to q_{rld}, and the value of q_{rsd} is constantly zero because tests are conducted during the night.

q_{sn} consists of the sensible heat flux due to natural wind q_{sa} (W m^{-2}), the sensible heat flux due to rainfall and snowfall q_{sf} (W m^{-2}), the sensible heat flux of drainage due to the road gradient q_{sr} (W m^{-2}), and the sensible heat flux of water dispersion due to passing vehicles q_{sv} (W m^{-2}), and q_{sn} is given by the following formula:

$$q_{sn} = q_{sa} + f(t)q_{sf} + q_{sr} + g(t)q_{sv}. \quad (23)$$

According to Newton's Law of Cooling, q_{sa} is expressed by the following formula:

$$q_{sa} = \alpha_{sa}(T_{wis} - T_a). \quad (24)$$

In this formula, α_{sa} is the coefficient of heat transfer between the atmosphere and the WIS layer on the road surface (W m^{-2} K^{-1}), and T_a is the air temperature (°C). α_{sa} is a function of the wind velocity v_w (m s^{-1}) and is given in formula (25) (Fujimoto et al., 2006).

$$\alpha_{sa} = 10.4v_w^{0.7} + 2.2 \quad (25)$$

On the assumption that the temperature of rain/snow is equal to T_a, q_{sf} is given by formula (26) using m_{wf} and m_{if}:

$$q_{sf} = \left(c_w m_{wf} + c_i m_{if}\right)T_a. \quad (26)$$

Because q_{sr} and q_{sv} are associated with water transfer, they are given by the following formulae using m_{sr} and m_{sv} respectively:

$$q_{sr} = 1000 m_{wr} c_w T_{wis} \quad (27)$$

$$q_{sv} = 1000 m_{wv} c_w T_{wis}. \quad (28)$$

In this formula, c_w and c_i are the specific heat of water and ice respectively (kJ kg^{-1} K^{-1}).

On the assumption that the latent heat as a result of phase changes of water, ice and salt is added to the heat balance of the WIS layer, q_{ln} is given by the following formula:

$$q_{ln} = q_{lwi} + q_{li} + q_{lw} + q_{ls} = m_{wi}L_{wi} + m_{il}L_i + m_{wl}L_w + m_{sl}L_s. \quad (29)$$

In the formula above, q_{lwi} is the latent heat flux of ice melting and water freezing (W m^{-2}), q_{li} is the latent heat flux of sublimation (W m^{-2}), q_{lw} is the latent heat flux of evaporation and condensation (W m^{-2}), q_{ls} is the latent heat flux of salt dissolution (W m^{-2}), L_i is the latent heat of sublimation (kJ kg^{-1}), L_w is the latent heat of evaporation and condensation (kJ kg^{-1}), and L_s is the latent heat of dissolution of salt (=−3.88/(58.44 × 10^{-3}) kJ kg^{-1}).

q_{vn} is the sum of the frictional heat flux of tires q_{vt} (W m^{-2}), the radiant heat flux of vehicles q_{vr} (W m^{-2}) and the sensible heat flux induced by vehicles q_{vw} (W m^{-2}), and is given by the following formula:

$$q_{vn} = g(t)\{q_{vt} + q_{vr} + q_{vw}\}. \quad (30)$$

Regarding q_{vt}, q_{vr} and q_{vw}, please refer to Fujimoto et al. (2012a).

3.3.2. Pavement

The heat balance inside the pavement is given by formula (31):

$$(\rho c)_p V_p \frac{\partial T_p}{\partial t} = q_{cp}. \quad (31)$$

In this formula, $(\rho c)_p$ is the volumetric heat capacity of pavement (J m^{-3} K^{-1}), V_p is the pavement elemental volume (m^3 m^{-2}), T_p is the pavement elemental temperature (°C) and q_{cp} is the conductive heat flux inside the pavement (W m^{-2}). According to Fourier' s Law of Conduction, q_{cp} is given by the following formula:

$$q_{cp} = -\lambda_p \frac{\partial T_p}{\partial z}. \quad (32)$$

In this formula, z is a vertical distance (m).

4. Field tests

4.1. Outline of the field tests

Fig. 3 shows the site of the field tests. A series of tests were conducted at Tomakomai Winter Test Track from evening to late at night for three days on January 21, 28 and 31 in 2013. The test track is a 2700-m-long circuit, and tests were implemented in a straight, level section paved with dense-graded asphalt.

The testing procedure is as follows: (i) After confirming that T_{ps} < 0 °C, a sprinkler truck sprinkles the 200-m-long test track with water; (ii) the surface water is completely frozen under low temperatures and the road surface is covered with ice film; (iii) salt spreading is applied to the ice-covered road surface; (iv) the temperature of the ice-covered surface is measured with a radiation thermometer on a vehicle; (v) samples of the ice film and the water film are taken at three fixed observation points; (vi) the salt concentration of the surface water is measured; (vii) fifty vehicles travel along the test track; and (vii) the steps from (iv) to (vii) are repeated until the total number of passing vehicles reaches 300 (i.e. 50 vehicles × 6 times). During or after a test, collected ice/water film samples are weighed and the thickness of the ice/water film is measured. The amount of residual salt on

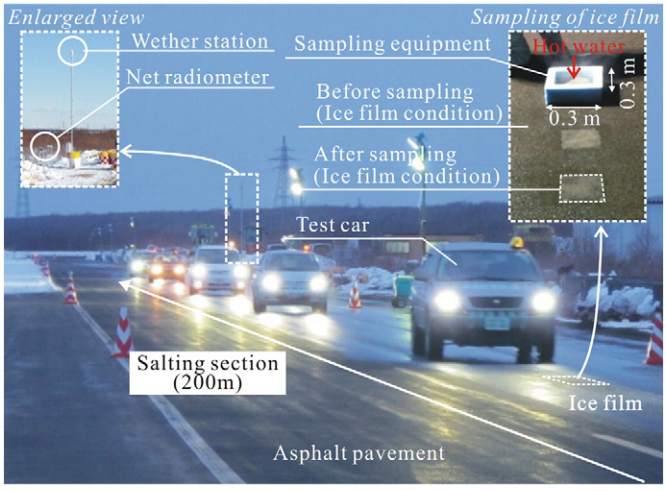

Fig. 3. Field test site.

the road surface is calculated using the values of the water film thickness and the salt concentration.

The method used for taking ice film samples is as follows: First, the water on the road surface is absorbed using a sheet of water-absorbing paper (20 mm × 20 mm). Second, an open-topped box is placed over the water absorbing paper on the ice film surface at the same place as the measurement of the water film as shown in the photo at the upper right of Fig. 3. The box is made of polystyrene foam (50 mm thick) except for the bottom, which is an aluminum board (1 mm thick). Third, hot water (about 90 °C) is poured into the box to melt the ice film on the road surface. The water absorbing paper absorbs water from melted ice film. Finally, after confirming that the ice film is completely melted, the water absorbing paper is removed and kept in a highly airtight plastic bag. In the same photo in Fig. 3, the road surface after collecting water from the ice film is shown to be dry, which means that an ice film sample was taken successfully. Water film samples were also taken by using water absorbing paper.

Test conditions used are as follows: The sodium chloride was used as the deicing agent (i.e. salt). The salt was sprinkled at a rate of 20 g m^{-2}. The traveling speed of the passing vehicles and the vehicle for measuring the road surface temperatures was 40 km h^{-1}.

As shown in the enlarged view at the upper left in Fig. 3, a meteorological instrument was installed for automatic recording of the air temperature, relative humidity, wind velocity, insolation flux, sky radiation flux and pavement temperature (at the depth of 50 mm) at 1-minute intervals.

4.2. Test results

The weather conditions and the flux of water dispersion due to passing vehicles (m_{wv}) during the tests are as explained below. Test results regarding the thickness of ice/water film, the surface temperature, the salt concentration and the amount of residual salt are described in the following section in connection with the results of calculation by the RSF-SV model.

4.2.1. Weather and traffic conditions

In Fig. 4(a), (b) and (c), weather monitoring results (T_a, v_w, related humidity RH_a (%) and q_{rld}) on January 21, 28 and 31, 2013 are shown. The time of the day when salt was sprinkled on the road surface is also shown. The weather was clear on all three days, with no precipitation when the tests were conducted. During the test, a round of 30-minute traveling of vehicles followed by 10-minute fixed-point observation was repeated. The hourly traffic volume was about 100 vehicles h^{-1}.

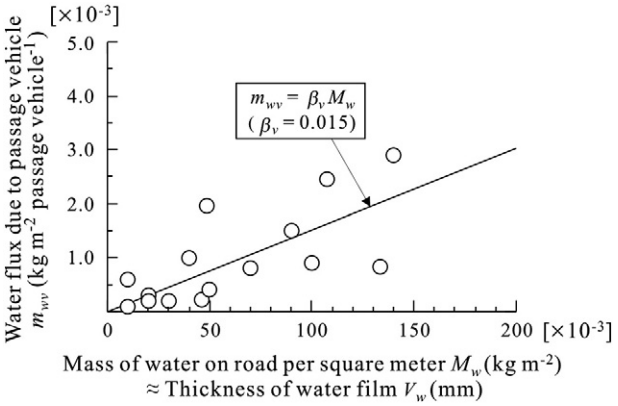

Fig. 5. The relationship between the flux of water loss due to passing vehicles and the thickness of the water film.

4.2.2. Flux of water dispersion due to passing vehicles

In formula (7) expressing the water balance on the road surface in the tests, m_{wf} is 0, m_{wl} is so small as to be negligible (5.3), m_{wr} is 0 in theory ($M_w/\rho_w < V_{wc}$ holds at all times during testing), and m_{wi} (i.e. refreeze due to decrease in T_a) is relatively small. From these values, it was presumed that the water loss on the road surface was dominantly caused by m_{wv}. Thus m_{wv}' (= m_{wv} per vehicle) was formulated on the assumption that M_w was reduced due to m_{wv}: m_{wv}' = (M_w after the vehicle passed by − M_w before 50 vehicles passes by) / 50.

Fig. 5 shows the relationship between m_{wv}' and M_w. m_{wv}' increased in proportion to the value of M_w. This relationship is expressed in the following formula:

$$m_{wv}' = \beta_v M_w. \tag{33}$$

In this study, β_v is called the coefficient of loss due to a passing vehicle (= 0.015 passing vehicle^{-1}). Because the traffic and road surface conditions were fixed in the tests, β_v can be regarded as a constant in this study. In fact, however, β_v is a coefficient that depends on various

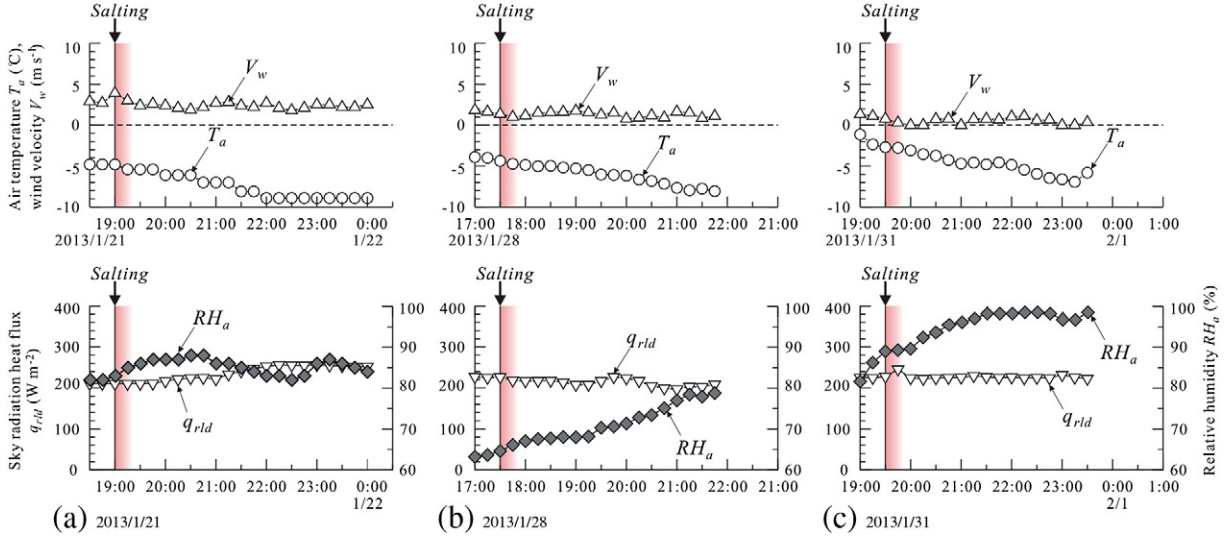

Fig. 4. Weather and traffic conditions in the field tests.

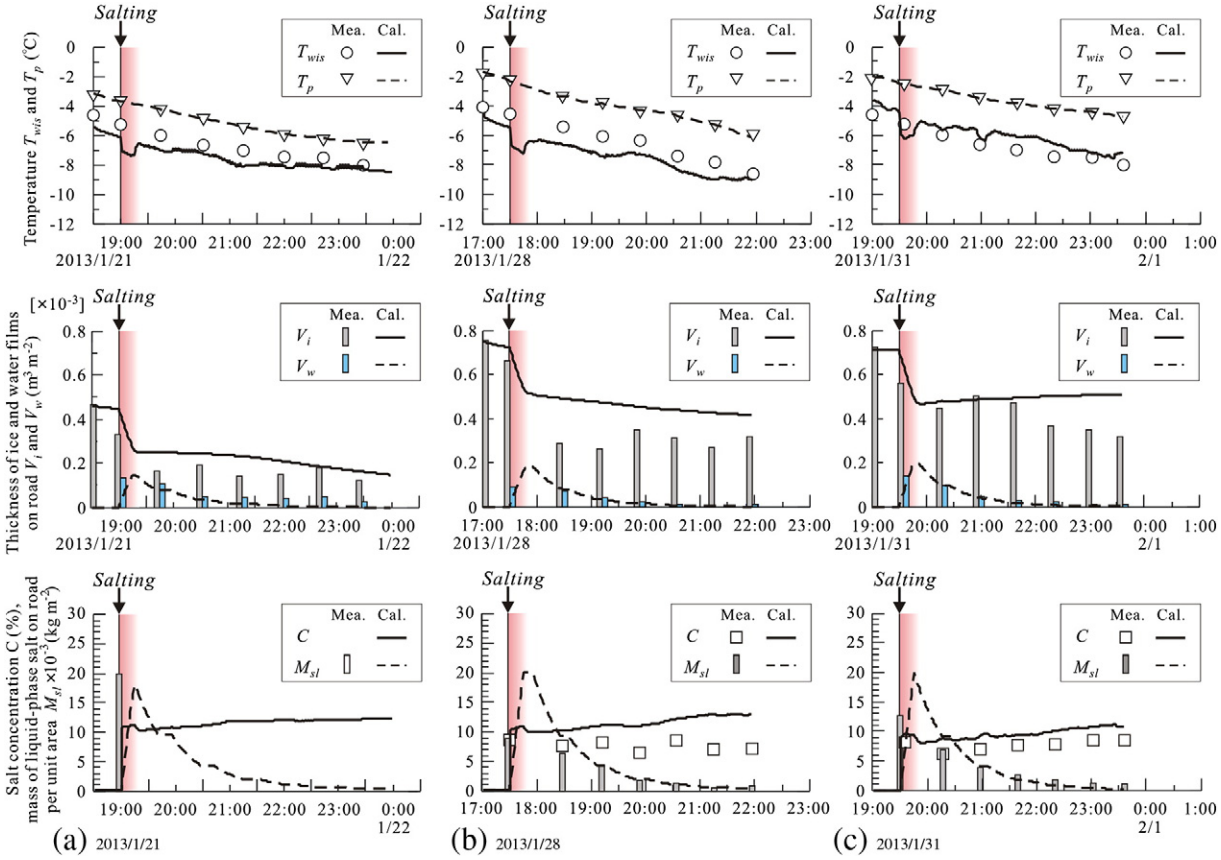

Fig. 6. Changes through time in the WIS layer temperature, the pavement temperature (at the depth of 50 mm), the thickness of ice/water film, the salt concentration, and the mass of liquid-phase salt (residual salt).

factors including vehicles, traveling speed, tires, pavement and road gradients. In order to use the RSF-SV model under various traffic/road conditions, quantitative evaluation of the features of β_v will be necessary in the future.

5. Validation of the RSF-SV model

5.1. Calculation conditions

Weather data inputted as the boundary condition of the top face of the analytical region (= the WIS layer) are automatically updated for every calculation interval (= about 1 s) by linear interpolation using the weather data obtained from observations every 1 min. Values measured with a thermocouple were given as the values on the bottom face of the analytical region. Salt was sprinkled in 30 min after the start of a test. To the dissolving flux (m_{sl}), 2.22×10^{-5} kg m^{-2} s^{-1} was given as a value that replicates the measured value. The dissolving flux is explained in more detail in 5.4 below.

5.2. Comparison of the test results and calculation results

Fig. 6(a), (b) and (c) show the results of tests conducted on January 21, 28 and 31, 2013, in terms of the time rate of change in T_{wis}, T_p (at the depth of 50 mm), V_i (= the thickness of ice film), V_w (= the thickness of water film), C and M_s. In the following, the index -m means measurement values, and the index -c means calculation values. Each of the values $V_{i\text{-}m}$, $V_{w\text{-}m}$, $C_{\text{-}m}$ and $M_{s\text{-}m}$ is the mean of values measured at the three observation points. The values of $C_{\text{-}m}$ and $M_{s\text{-}m}$ were not measured on January 21.

5.2.1. Temperatures of the WIS layer and the pavement

The test results regarding T_{wis} and T_p are explained as follows. On each of the three days when tests were conducted, the values of $T_{wis\text{-}m}$ and $T_{p\text{-}m}$ decreased with time.

The value of $T_{wis\text{-}c}$ dropped drastically immediately after the application of salt. As explained in Step 2, 2.1 above, this significant drop in $T_{wis\text{-}c}$ is due to the melting heat and the heat of salt dissolution (i.e. heat absorption by sodium chloride) which are generated when salt contacts with ice. The subsequent rise in $T_{wis\text{-}c}$ is due to the heat conducted from the surroundings. Although the calculation values and the measurement values (i.e. $T_{wis\text{-}c}$ and $T_{wis\text{-}m}$) slightly differ depending on the differences in the physical properties of pavement, the path used by passing vehicles and micrometeorological conditions along the road, the RSF-SV model replicated the temperatures of the WIS layer to a considerable extent.

5.2.2. The thickness of the ice film and the water film

The measurement values of the ice/water film thickness are as explained below. After the application of salt, $V_{i\text{-}m}$ decreased by 0.1–0.3 mm. After that, the value of $V_{i\text{-}m}$ only slightly fluctuated and did not change greatly. The $V_{w\text{-}m}$ generated as a result of ice film melting and decreased with time.

Regarding the calculation values, $V_{i\text{-}c}$ decreased by 0.2 mm after the application of salt. The value only slightly decreased in the tests on January 21 and 28 and slightly increased in the test on January 31. The slight decrease and increase in the value of $V_{i\text{-}c}$ after the application of salt are mainly due to m_{il}. On January 31, the value of RH_a remained relatively high, which caused sublimation from the air to the WIS layer ($m_{il} > 0$) while sublimation from the WIS layer to the air took place ($m_{il} < 0$) on the other two days of testing. Contrary to the calculation results, $V_{i\text{-}m}$

Table 1
Mean absolute errors of calculation values.

	$V_{i\text{-}c}$	$V_{w\text{-}c}$	$C_{\text{-}c}$	$M_{sl\text{-}c}$
2013/1/21	0.06	0.04	–	–
2013/1/28	0.12	0.02	3.12	3.02
2013/1/31	0.08	0.02	1.88	2.32

tends to decrease with time in the test on January 31. These systematic discrepancies between $V_{i\text{-}c}$ and $V_{i\text{-}m}$ may be caused by differences between the calculated ρ_{va} and actual ρ_{va} near the road surface. In this model, ρ_{va} is calculated from the air temperature and related humidity obtained at the height of 6 m in the test field. Actually, frost occurred at various locations in the test field at that time. However, increases of ice on the road were not visually observed.

Regarding $V_{w\text{-}c}$, a water film thickness of 0.2 mm was generated immediately after the application of salt, and then the thickness decreased exponentially.

Although the values of $V_{i\text{-}m}$ vary due to the texture and the unevenness on the test track surface and thus it is difficult to precisely compare the calculation results and the measurement results, calculated values ($V_{i\text{-}c}$ and $V_{w\text{-}c}$) replicated measurement values to a great extent. Table 1 shows the mean absolute error (MAE)s of $V_{i\text{-}c}$ and $V_{w\text{-}c}$.

5.2.3. Salt concentration and residual salt

On January 28 and 31, the values of salt concentration ($C_{\text{-}m}$) were in the range of 6.5–8.7% and 6.2–8.5% respectively. The values of $M_{sl\text{-}m}$ were 9.0 g m^{-2} and 12.6 g m^{-2} immediately after the application of salt, dropped in an exponential manner, and became almost zero at the end of the test.

The value of $C_{\text{-}c}$ increased to the level that corresponds to the salt concentration at the temperature of the WIS layer (T_{wis}) immediately after the application of salt. After that, the value of $C_{\text{-}c}$ increased slightly as the value of T_{wis} gradually decreased with time on all the three days. Although the values of $C_{\text{-}c}$ are higher than the values of $C_{\text{-}m}$, the calculation values replicated the measurement values to a substantial extent. We estimated that these results are attributed to the dilution of the salt solution due to melting ice on the road during sampling. The values of $M_{sl\text{-}c}$ were in good agreement with the values of $M_{sl\text{-}m}$. MAEs of $C_{\text{-}c}$ and $M_{sl\text{-}c}$ are listed in Table 1.

5.3. Heat, water, ice and salt transfer

The heat, water, ice and salt balance is examined below by focusing on the calculation results regarding the test on January 31, 2013. From the top to the bottom of Fig. 7, the balances of ice, water, salt and heat are shown. In the graphs regarding the balances of ice, water and salt, the horizontal axis shows the accumulated total mass per square meter. In the graphs for the heat balance, the horizontal axis shows the ratio of each heat flux to the total absolute values of all heat fluxes. In the following, the index * means the accumulated total mass or the ratio. The values of m_{if}, m_{iv}, m_{wf}, m_{wr}, m_{sr}, q_{rsn}, q_{sf}, and q_{sr} were always 0 in the analysis and thus are not shown in the graphs.

Regarding the ice balance, during the test, there were ice losses of $m_{wi}{}^*$ (=−0.212 kg m^{-2}) and ice gain of $m_{il}{}^*$ (=0.027 kg m^{-2}). The amount of change in M_i during the test (ΔM_i) was −0.185 kg m^{-2} (i.e. 0.651 kg m^{-2} (at the beginning of the test)–0.466 kg m^{-2} (at the end of the test)).

As for the water balance, while water was supplied by $m_{wi}{}^*$ (=0.212 kg m^{-2}), most of the water was lost by $m_{wv}{}^*$ (=−0.215 kg m^{-2}). The gain of $m_{wl}{}^*$ was small (=0.002 kg m^{-2}). During the test, the amount of change in the value of M_w (ΔM_w) was 0.001 kg m^{-2}.

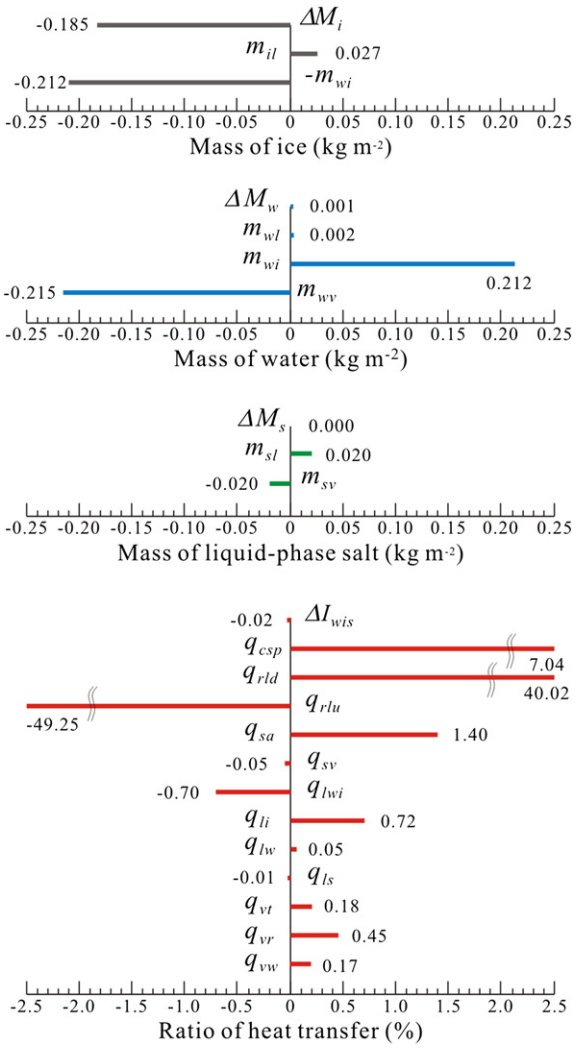

Fig. 7. Ice, water, salt and heat balance (Jan. 31, 2013).

The supply of salt due to $m_{sl}{}^*$ (=0.020 kg m^{-2}) was balanced out by the loss of $m_{sv}{}^*$ (=−0.020 kg m^{-2}).

Regarding the heat balance, $q_{rlu}{}^*$ (=−49.25%) affected the road surface conditions as a dominant negative factor that contributed to a drop in T_{wis}, or to freezing of the surface. $q_{rld}{}^*$ (=40.02%) and $q_{csp}{}^*$ (=7.04%) were dominant positive factors that contributed to a rise in T_{wis} or to melting of ice. The heat fluxes attributable to vehicles, namely $q_{vt}{}^*$ (=0.18%), $q_{vr}{}^*$ (=0.45%) and $q_{vw}{}^*$ (=0.17%), were positive values, and the sum of these fluxes q_{vn} was 0.80%. Another positive factors were $q_{sa}{}^*$ (=1.40%), q_{li} (=0.72%) and q_{lw} (=0.05%). In ascending order, the negative factors affecting the road surface are q_{lwi} (=−0.70%), q_{sv} (=−0.05%) and q_{ls} (=−0.01%).

5.4. The effects of the dissolving flux on the road surface freeze analysis

For the purpose of examining the effects of the melting flux m_{sl} on T_{wis}, V_i, V_w and M_{sl}, sensitivity analysis was conducted regarding the result of the test on January 31 (Fig. 8). The sensitivity analysis was conducted under three different conditions of m_{sl}: $m_{sl} = 0.56 \times 10^{-5}$, 2.22×10^{-5}, or 6.67×10^{-5} kg m^{-2} s^{-1}. These conditions are respectively called Case-S, Case-M and Case-H below. In Case-S, Case-M and Case-H, the length of time required for complete dissolution of salt is 60, 15 and 5 min respectively under the condition that $m_{sf} = 0.02$ kg m^{-2}.

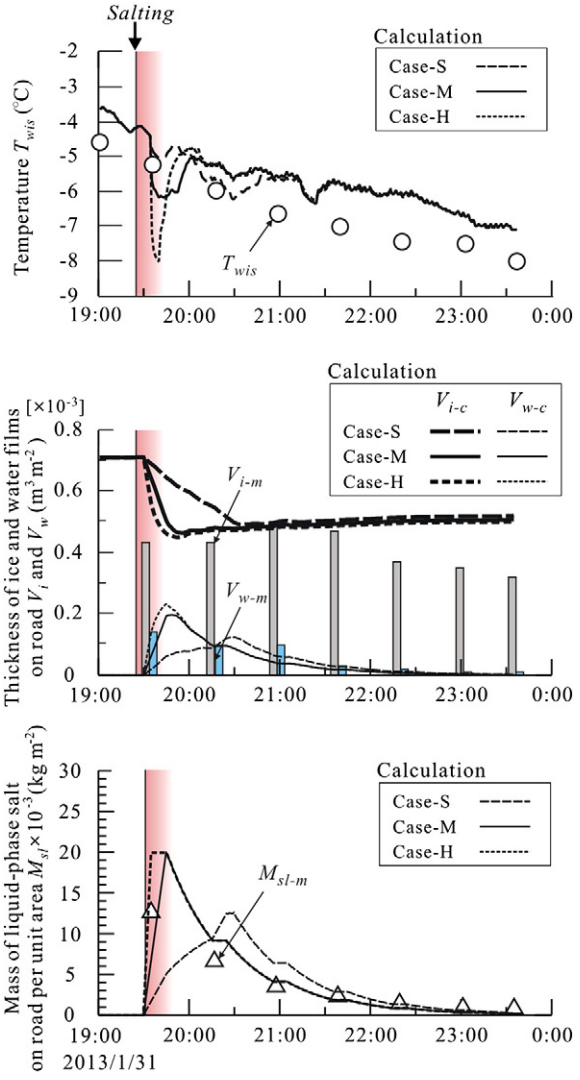

Fig. 8. The effects of the melting flux on the analytical solutions of road surface freeze analysis (Jan. 31, 2013).

A drop in the value of T_{wis} immediately after the application of salt becomes more remarkable as the value of m_{sl} becomes larger. In Case-H, the value of T_{wis} decreased to around −8 °C. This decrease in T_{wis} is caused by the latent heat of salt dissolution and the latent heat of ice melting (i.e. negative heat fluxes). When the value of m_{sl} becomes larger, high latent heat affects the WIS layer in a shorter period of time. There are no large differences between Case-M and Case H regarding V_i and V_w. In Case-S, however, the calculated rate of decrease in V_i and the calculated rate of increase in V_w immediately after the application of salt are smaller than the measured rates, and thus the changes in the measurement values with time are not replicated in the model. Regarding M_{sl}, the measurement values and calculation values in Case-M and Case-H decreased exponentially immediately after the application of salt. But in Case-S, the maximum calculation value was shown at 20:30, and thus the changes with time in the calculated value of M_{sl} are not in good agreement with the measurement values. In the analysis scheme used in this study, analytical solutions diverged when m_{sl} was larger than 6.67×10^{-5} kg m^{-2} s^{-1}. In other words, there were alternating condensation of a salt solution due to a rapid fall in temperature (i.e. freezing) and dilution of the salt solution due to a rapid rise in temperature (i.e. melting).

6. Conclusions

This study clarified the relationship between the water/salt transfer due to passing vehicles and the thickness of the water film on the road surface. On the basis of the understanding of this relationship, a new Road Surface Freeze prediction model based on heat, water and salt balance that takes into account the effects of Salting and passing Vehicles (RSF-SV model) was developed. The validity of the model was examined through comparison of the calculation results and the field test results. The heat, water, ice and salt transfer on the road surface due to passing vehicles after salt spreading was examined in detail. Furthermore, sensitivity analysis was conducted for examining the effects of the salt dissolution rate on the snow and ice on the road surface as well as on the residual salt.

The findings in this study are enumerated below:

(1) The flux of water dispersion due to passing vehicles increases linearly with an increase in the thickness of the water film on the road surface. The relationship between the flux of water dispersion due to passing vehicles and the thickness of the water film on the road surface was formulated.
(2) The RSF-SV model was useful for calculating the time rate of change in the amount of residual salt, the salt concentration, the thickness of ice/water film, and the temperature of the WIS layer during simultaneous phase transition of water, ice and salt after the application of salt on the ice-covered road surface.
(3) In the water balance on the ice-covered surface after salt sprinkling, a large water loss is caused by the flux of water dispersion due to passing vehicles, although water loss also depends on traffic conditions.
(4) In the analysis of road surface freezing after the application of salt, valid calculation results were obtained by setting the values of dissolving flux to 2.22×10^{-5}–0.67×10^{-5} kg m^{-2} s^{-1}.

Although the weather and traffic conditions were limited in the tests, it was proved that the RSF-SV model developed in this study was available for taking into account the effects of passing vehicles and salt application.

Tests and analysis will be continued in the future for the purpose of quantifying the flux of water and solid salt dispersion due to passing vehicles and the dissolving flux, of expanding the versatility of the model, and of applying the model to actual roads. When the RSF-SV model is completed, it will be possible to evaluate the conditions of snow and ice on the road surface after the application of salt, the salt concentration, and the residual salt on the road surface. Completion of this model is expected to help optimize the application of deicing agents.

Acknowledgments

This work was supported by JSPS KAKENHI Grant Number 23710191.

Appendix A

List of symbols

C	salt concentration (−)
c_i	specific heat of ice (kJ kg^{-1} K^{-1})
c_w	specific heat of water (kJ kg^{-1} K^{-1})
$f(t), g(t)$	discriminant variables of the flux that is generated and lost due to passing vehicles
k	coefficient of runoff velocity (s^{-1})
L_i	latent heat of sublimation (kJ kg^{-1})
L_s	latent heat of dissolution of salt (kJ kg^{-1})
L_w	latent heat of evaporation and condensation (kJ kg^{-1})
L_{wi}	latent heat of melting and freezing (kJ kg^{-1})
M_i	mass of ice (kg m^{-2})
m_{if}	snowfall flux (kg m^{-2} s^{-1})

m_{il} sublimation flux (kg m^{-2} s^{-1})
m_{iv} flux of ice loss (i.e. dispersion and wear of ice) due to passing vehicles (kg m^{-2} s^{-1})
m_{wi} melting and freezing flux (kg m^{-2} s^{-1})
M_s mass of salt (kg m^{-2})
m_{sf} salt spreading flux (kg m^{-2} s^{-1})
m_{sl} dissolving flux (kg m^{-2} s^{-1})
M_{sl} mass of liquid-phase salt (kg m^{-2})
M_{ss} mass of solid-phase salt (kg m^{-2})
M_w mass of water (kg m^{-2})
M_{wis} mass per unit area of WIS layer (kg m^{-2})
m_{wf} rainfall flux (kg m^{-2} s^{-1})
m_{wl} flux of evaporation and condensation (kg m^{-2} s^{-1})
m_{wr} flux of road drainage (kg m^{-2} s^{-1})
m_{wv} flux of water dispersion due to passing vehicles (kg m^{-2} s^{-1})
m_{wv}' water dispersion due to a passing vehicle (kg m^{-2} passing vehicle^{-1})
m_{sr} flux of salt discharged from the road surface (kg m^{-2} s^{-1})
m_{ssv} flux of solid-phase salt dispersion due to passing vehicles (kg m^{-2} s^{-1})
m_{sv} flux of salt loss due to passing vehicles (i.e. dispersion into the atmosphere and adherence to vehicle bodies) (kg m^{-2} s^{-1})
q_{net} net heat balance of the WIS layer (W m^{-2})
q_{cp} conductive heat flux inside the pavement (W m^{-2})
q_{csp} flux of pavement heat (i.e. heat conducted between WIS layer on road surface and pavement) (W m^{-2})
q_{li} latent heat flux of sublimation (W m^{-2})
q_{ln} flux of net latent heat (W m^{-2})
q_{ls} latent heat flux of salt dissolution (W m^{-2})
q_{lw} latent heat flux of evaporation and condensation (W m^{-2})
q_{lwi} latent heat flux of ice melting and water freezing (W m^{-2})
q_{rld} flux of long-wave sky radiation (W m^{-2})
q_{rlu} flux of long-wave radiation on road surface (W m^{-2})
q_{rn} flux of net radiant heat (W m^{-2})
q_{rsd} flux of short-wave radiation (W m^{-2})
q_{rsu} reflection component of q_{rsd} (W m^{-2})
q_{sa} sensible heat flux due to natural wind (W m^{-2})
q_{sf} sensible heat flux due to rainfall and snowfall (W m^{-2})
q_{sn} flux of net sensible heat (W m^{-2})
q_{sr} sensible heat flux of drainage due to road gradient (W m^{-2})
q_{sv} sensible heat flux of water dispersion due to passing vehicles (W m^{-2})
q_{vn} flux of net vehicle heat (W m^{-2})
q_{vr} radiant heat flux of vehicles (W m^{-2})
q_{vt} frictional heat flux of tires (W m^{-2})
q_{vw} sensible heat flux induced by vehicles (W m^{-2})
r_c thermal contact resistance generated in interface between pavement surface and WIS layer (m^2 K W^{-1})
RH_a related humidity (%)
t time (s)
T_a air temperature (°C)
T_f freezing point (°C)
T_p pavement elemental temperature (°C)
T_{ps} representative temperature of pavement layer which means temperature of pavement $V_{ps}/2$ below the interface between WIS layer and pavement layer (°C)
T_{wis} temperature of WIS layer (°C)
v_{fi} snowfall intensity (m s^{-1})
v_{fw} rainfall intensity (m s^{-1})
V_p pavement elemental volume (m^3 m^{-2})
V_{ps} thickness of the pavement surface elemental layer (m^3 m^{-2})
v_w wind velocity (m s^{-1})
V_{wc} critical water film thickness on the surface (m^3 m^{-2})
V_{wis} volume of WIS layer (m^3 m^{-2})
v_{ws} wind velocity (m s^{-1})
z vertical distance (m)
α_{il} bulk sublimation coefficient (m s^{-1})
α_{sa} coefficient of heat transfer between atmosphere and WIS layer on road surface (W m^{-2} K^{-1})
α_{wl} bulk coefficient of evaporation and condensation (m s^{-1})
β_v coefficient of loss due to a passing vehicle (passing vehicle^{-1})
ε_{wis} emissivity of WIS layer surface (−)
θ_a air content by volume in WIS layer (−)
θ_i ice content by mass (−)
λ_p thermal conductivity of pavement (W m^{-1} K^{-1})
λ_{wis} thermal conductivity of WIS layer (W m^{-1} K^{-1})
$(\rho c)_p$ volumetric heat capacity of pavement (J m^{-3} K^{-1})
$(\rho c)_{wis}$ volumetric heat capacity of WIS layer (J m^{-3} K^{-1})
ρ_{snow} snow density (kg m^{-3})
ρ_{va} atmospheric water vapor concentration (kg m^{-3})
ρ_{vs} road surface water vapor concentration (kg m^{-3})
ρ_w water density (kg m^{-3}).
σ *Stefan–Boltzmann* constant (W m^{-2} K^{-4})
ϕ falling rate of water vapor concentration (−)
ΔM_i amount of change in M_i during the test
ΔM_w amount of change in M_w during the test
Δt_v short time for m_{wv}' (s passing vehicle^{-1})
-m, *-c* suffixes expressed as measurement and calculation values
* accumulated total mass or the ratio

References

Bouilloud, L., Martin, E., 2006. A coupled model to simulate snow behavior on roads. J. Appl. Meteorol. 45, 500–516.
Cengel, Y.A., 1998. Heat Transfer: A Practical Approach. Tata Mc-Graw-Hill Publishimg Company Limited, p. 968.
Chapman, L., Thornes, J.E., 2005. The influence of traffic on road surface temperatures: implications for thermal mapping studies. Meteorol. Appl. 12, 371–380.
Chapman, L., Thornes, J.E., Bradley, A.V., 2001. Modeling of road surface temperatures from a geographical parameter database. Part 1: statistical. Meteorol. Appl. 8, 409–419.
Crevier, L.P., Delage, Y., 2001. METRo: a new model for road-condition forecasting in Canada. J. Appl. Meteorol. 40, 2026–2037.
Fujimoto, A., Watanabe, H., Fukuhara, T., Sato, T., Nemoto, M., Mochizuki, S., Kishii, T., 2006. Heat and water vapor transfer between atmosphere and pavement surface under dry, wet, ice plate and packed snow sates. J. Snow Enj. Jpn. 22, 220–228.
Fujimoto, A., Watanabe, H., Fukuhara,, 2007. Thermal contact resistance between snow/ice layer and pavement surface. J. Jpn. Soc. Civ. Eng. 63, 156–165.
Fujimoto, A., Watanabe, H., Fukuhara, A., 2008. Effects of vehicle heat on road surface temperature of dry condition. Proc. 14th Standing Int. Road Weather Conf., Standing International Road Weather Commission, Prague, Czech Republic, p. ID05.
Fujimoto, A., Saida, A., Fukuhara, T., 2012a. A new approach to modeling-vehicle-induced heating and its thermal effect on road surface temperature. J. Appl. Meteorol. Climatol. 51, 1980–1993.
Fujimoto, A., Saida, A., Fukuhara, T., 2012b. Analysis of freezing of sodium chloride solution on road surface. Proceedings of the 7th International Conference on Snow Engineerin, 7, pp. 415–426.
Greenfield, T.M., Takle, E., 2006. Bridge frost prediction by heat and mass transfer methods. J. Appl. Meteorol. 45, 517–525.
He, C., Fukuhara, T., Takano, Y., Nanjyo, M., 2003. Heat, moisture and salt movement in a soil containing a salt accumulated layer due to watering and evaporation. J. Hydraul. Coast. Environ. Eng. 747 (II-65), 15–28.
Jansson, C., Almkvist, E., amd Janson, P.E., 2006. Heat balance of an asphalt surface: observations and physically-based simulations. Meteorol. Appl. 13, 203–212.
Knollhoff, D.S., Takle, E.S., Gallus Jr., W.A., Burkheimer, D., McCauley, D., 2003. Evaluation of a frost accumulation model. Meteorol. Appl. 10, 337–343.
Rayer, P.J., 1987. The Meteorological Office forecast road surface temperature model. Meteorol. Mag. 116, 180–191.
Sass, B.H., 1992. A numerical model for prediction of road surface temperature and ice. J. Appl. Meteorol. 31, 1499–1506.
Shao, J., 1990. A Winter Road Surface Temperature Prediction Model with Comparison to Others. The University of Birmingham, pp. 1–245.
Takahashi, N., Tokunaga, R.A., Asano, M., Ishikawa, N., 2006. Developing a method to predict road surface temperatures: applying heat balance model considering traffic volume. Proc. 13th Standing Int. Road Weather Conf., Standing International Road Weather Commission, Torino, Italy, 13, pp. 58–66.
Thornes, J.E., 1984. The Prediction of Ice Formation on Motorways. (Ph.D. thesis) University College, London, pp. 1–392.